



WEDNESDAY SLIDE CONFERENCE 2013-2014

Conference 16

19 February 2014

**CASE I: 11-V62 (JPC 4001100).**

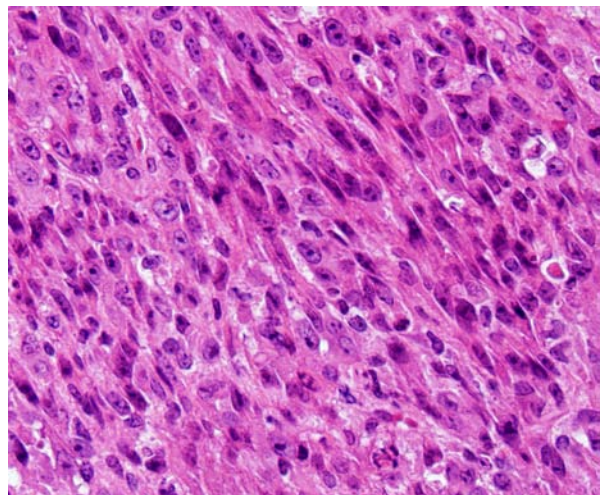
**Signalment:** 1.5-year-old genetically-modified mouse (*Mus musculus*). Strain is mdx  $-/-$  on C57Bl6/J background.

**History:** Animal was reported for hind limb paralysis/paresis, with slow to absent withdrawal reflexes. The left side was more severely affected than the right side. The animal had also been on

oral sildenafil (Viagra; dose and duration not given) and had been anesthetized for an echocardiogram the week before coming to necropsy. The mouse was submitted for necropsy and though the investigative group collected most tissues, the carcass with a peritoneal mass was submitted to the Veterinary Diagnostic Lab for histology.



1-1. Vertebral column, epaxial musculature, and overlying haired skin, mouse: The epaxial musculature is effaced by a mesenchymal neoplasm which infiltrates the spinal canal and elevates the overlying haired skin. (HE 0.63X)



1-2. Vertebral column, epaxial musculature, and overlying haired skin, mouse: Neoplastic cells are arranged in broad streams and spindle shaped with large nuclei. Mitotic figures are common. (HE 320X)

**Gross Pathology:** The gross necropsy was not performed by the Veterinary Diagnostic Lab. Veterinary Services reported that an older adult mouse, well-groomed and in good body condition (adequate fat stores), was euthanized by the investigative group with an overdose of isoflurane. In the abdominal cavity, a pale tan soft tissue mass was found adhered bilaterally in the region of the lumbosacral spine, appearing to fuse with the spine.

Peritoneal cavity: Lumbosacral soft tissue mass.

**Histopathologic Description:** Lumbosacral spine mass: In a section of body wall with overlying haired skin, lumbar muscle and spinal cord, is a very large (~1 cm diameter at widest point), densely cellular, unencapsulated tumor. It is invasive, infiltrating through lumbar musculature, lymph node, and into the spinal canal. The tumor cells vary in shape, ranging from small round cells with scant cytoplasm to spindle-shaped cells. Occasional mitotic figures are seen. The cells form densely packed bundles and streams, arranged in medium-sized alveolar-type structures. Cell borders are indistinct and there is marked anisocytosis and anisokaryosis. “Strap” cells appear as a single elongated nucleus or series of nuclei lined up across a band of elongated cytoplasm. “Paddle” cells are hypereosinophilic cells that appear to sit on a stalk and occupy a cleared space and are particularly evident where the tumor borders and infiltrates skeletal muscle. The tumor effaces one side of the spinal canal, displacing the cord laterally and causing compression of the spinal nerve, which shows some axon loss, vacuolization, and smaller caliber fibers compared to the contralateral nerve. The spinal cord neuropil shows some mild gliosis and neuronal cell death on the affected side.

**Contributor’s Morphologic Diagnosis:** Lumbar musculature: Rhabdomyosarcoma with invasion into the spinal canal and spinal cord compression.

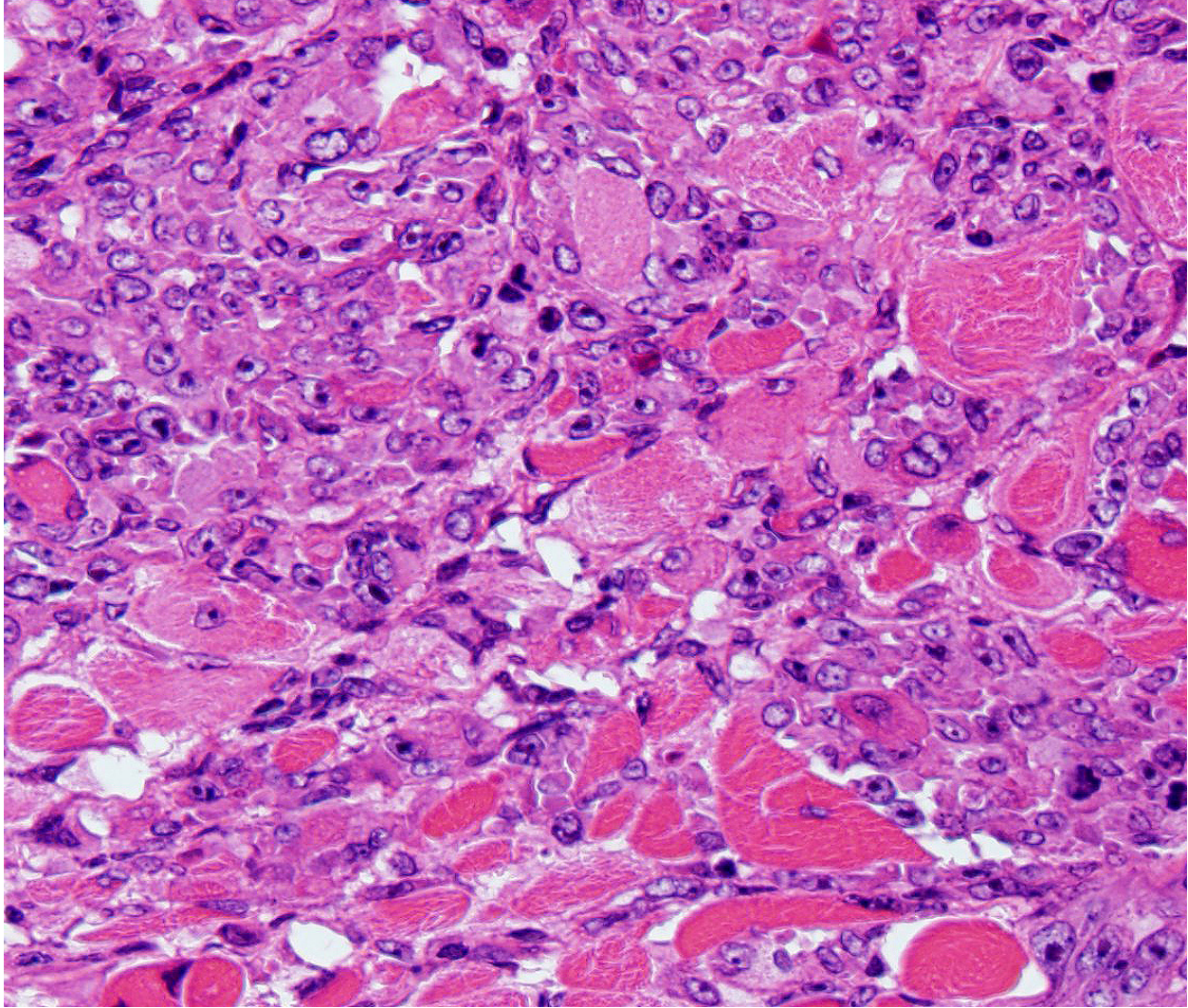
Spinal cord: Compressive unilateral leukomalacic myelitis, white matter degeneration and regeneration, and spinal ganglia neuritis, chronic-active.

**Contributor’s Comment:** Duchenne’s muscular dystrophy (DMD) in humans is due to defective

or absent dystrophin, a protein integral to structural stability of myofibers. Dystrophin is a large protein (427 kDa) on the inner face of the sarcolemma that binds with cytoskeletal f-actin and the transmembrane protein beta-dystroglycan as part of a complex, multimolecular unit that mediates signaling between the intracellular cytoskeleton and the extracellular matrix. Duchenne’s muscular dystrophy is the most common lethal inherited disorder of children (1/3500 newborn males).<sup>11</sup> The disease shows X-linked recessive inheritance. There are no signs at birth. As affected children age, they develop weakness, hyperlordosis with wide-based gait, and hypertrophy of weak muscles. The disease follows a progressive course, with eventual reduced muscle contractility, bladder/bowel dysfunction, and death due to respiratory failure. Two cases of rhabdomyosarcoma in DMD patients has been reported, one alveolar and one embryonal,<sup>1</sup> though the incidence does not appear to exceed that of the general population.<sup>3</sup> There are no therapies currently available, though stem cells and viral gene therapy show some promise.<sup>10</sup>

The most effective model for characterizing the structure and function of dystrophin and possible therapeutic interventions for DMD is the *mdx* mouse.<sup>1</sup> The official nomenclature of *mdx* mice is C57BL/10Scsn-*Dmd*<sup>*mdx*</sup>/J. A point mutation in exon 23 of the x-linked dystrophin gene (*dmd*) creates a nonsense mutation that converts cytosine to thymine. This substitution replaces a glutamine codon with a termination codon, causing abnormal production, and/or reduced stability of truncated gene products. In *mdx* mice, skeletal muscle has normal histologic features until about 3 weeks of age.<sup>4</sup> It then undergoes progressive degeneration and necrosis; small caliber fibers with central nuclei can be observed as part of the regenerative response.<sup>4</sup> In mice, the mutated dystrophin gene does not manifest with severe muscular dystrophy, as it does in humans, due to compensatory responses by utrophin. It does however have a somewhat shortened lifespan,<sup>1</sup> though not as dramatic as in humans. In mice with both utrophin and dystrophin knocked out, there is more severe disease and premature death.

In our facility and others,<sup>1</sup> *mdx* mice show a tendency toward developing spontaneous rhabdomyosarcomas. They can occur on the distal limb or the trunk, as in this case. There is no limb predilection.<sup>1</sup> Rhabdomyosarcoma is a



1-3. Vertebral column, epaxial musculature, and overlying haired skin, mouse: At the edge of the neoplasm, neoplastic cells surround, separate, and replace remaining skeletal muscle. (HE 320X)

malignant tumor of striated muscle that is, in veterinary medicine, divided into four major histologic categories: embryonal, botryoid, alveolar, and pleiomorphic {Mueuten, 2002 #129}. Diagnostic features of rhabdomyosarcoma include elongate “strap” cells, “racket” cells, as well as cross striations which can be highlighted with phosphotungstic acid-hematoxylin stain (PTAH).<sup>5</sup> These tumors can also be labeled with myosin, actin, desmin, vimentin, BB creatine kinase, NCAM, IFG-II and TGF-Beta.<sup>5</sup> Rhabdomyosarcoma in mice has been shown to express the myogenic differentiation factors myogenin, MyoD, and the muscle intermediate filament protein desmin.<sup>3</sup> It is speculated that *mdx* mice are predisposed because of the lifelong continuous myofiber degeneration and regeneration, which is associated with continuous

and massive activation and proliferation of satellite cells (muscle progenitor cells), increasing the chance of developing random and spontaneous mutations.<sup>2</sup> Inactivation of p53 is a primary event in *mdx* rhabdomyosarcoma.<sup>3</sup>

Other animal models of DMD include dogs, cats, zebrafish, and *C. elegans*.<sup>2</sup> In dogs, there is an X-linked muscular dystrophy in several breeds, including golden retrievers, Rottweilers, German short-haired pointers, and beagles. The manifestation in golden retriever is most closely homologous model of DMD. In this breed, the disease results from a single base pair change in the 3' consensus splice site of intron 6, which leads to skipping of exon 7 and a misaligned reading frame in exon 8 that causes a premature stop codon.<sup>11</sup> The myocardium is more severely

affected in the golden retriever than in other animal models, though this feature of the disease course makes it much closer to the manifestation in humans.<sup>11</sup> Cats have a hypertrophic feline muscular dystrophy that has limited similarity to DMD. In cats, the disease is due to a 200 kb deletion of the dystrophin gene, which causes a hypertrophic muscular dystrophy.<sup>11</sup> Affected cats typically have elevated creatine kinase in the blood by 4-5 weeks of age, before apparent muscle involvement, which can be seen at 10-14 weeks.<sup>11</sup> Affected cats die of esophageal compression by a hypertrophic diaphragm, or of the inability to drink due to glossal hypertrophy.<sup>11</sup> Zebrafish and *C. elegans* express a dystrophin homologue that is used for gene analysis and drug discovery. There are no primate models of DMD.<sup>11</sup>

**JPC Diagnosis:** 1. Vertebral body and epaxial musculature: Rhabdomyosarcoma.  
2. Spinal cord: Leukomalacia, focally extensive, moderate.

**Conference Comment:** The contributor provides a thorough overview of rhabdomyosarcoma in this transgenic mouse model, as well as summarizing various animal models of DMD (see table 1). Readers may also wish to review the conference proceedings for WSC 2012-2013, conference 16, case 3 for a general discussion of rhabdomyosarcoma. As expected, neoplastic cells in this case expressed strong, multifocal positive cytoplasmic immunoreactivity for desmin, while histochemical staining with PTAH demonstrated rare islands of neoplastic cells with cross striations.

Table 1: Animal models of muscular dystrophy.<sup>2,6,7-9,11</sup>

Model	Species	Defect	Other
X-linked muscular dystrophy (mdx; Duchenne's-like)	mdx mouse	X-linked dystrophin defect	No muscle wasting due to compensatory responses by utrophin
Human classical congenital muscular dystrophy	dy+/dy+ mouse	Autosomal recessive laminin alpha 2 (merosin) deficient	Loss of myelin in ventral nerve roots

X-linked muscular dystrophy (xmd; Duchenne's-like)	Dog	X-linked dystrophin defect	Best characterized in golden retriever; myocardium more severely affected than other muscles
Hypertrophic feline muscular dystrophy	Cat	X-linked dystrophin defect	Protruding tongue, bunny-hopping gait; malignant hyperthermia-like syndrome
Hereditary muscular dystrophy	Chicken	Autosomal dominant defect in Ubiquitin ligase gene (WWP1)	Superficial pectoralis (large breast muscle); affects type II muscle fibers
Ovine muscular dystrophy	Merino sheep	Autosomal recessive	Australia
Muscular dystrophy	Meuse-Rhine-Yssel cattle (Netherlands); rarely in Holstein-Friesians	Probably autosomal recessive	Usually affects diaphragm

**Contributing Institution:** University of Washington  
Department of Comparative Medicine  
<http://depts.washington.edu/compmed/index.html>

**References:**

1. Chamberlain JS, Metzger J, Reyes M, Townsend D, Faulkner JA. Dystrophin-deficient mdx mice display a reduced life span and are susceptible to spontaneous rhabdomyosarcoma. *FASEB J.* 2007;21:2195-2204.
2. Collins CA, Morgan JE. Duchenne's muscular dystrophy: animal models used to investigate pathogenesis and develop therapeutic strategies. *Int J Exp Pathol.* 2003;84:165-172.

3. Fernandez K, Serinagaoglu Y, Hammond S, Martin LT, Martin PT. Mice lacking dystrophin or alpha sarcoglycan spontaneously develop embryonal rhabdomyosarcoma with cancer-associated p53 mutations and alternatively spliced or mutant Mdm2 transcripts. *Am J Pathol*. 2010;176:416-434.
4. The Jackson Laboratory, JAX mice database-C57BL/10ScSn-Dmd<sup>mdx</sup>/J. <http://jaxmice.jax.org/strain/001801.html>.
5. Maronpot RR. *Pathology of the Mouse: Reference and Atlas*. Vienna, IL: Cache River Press; 1999:637-642.
6. Matsumoto H, Maruse H, Inaba Y, et al. The ubiquitin ligase gene (WWP1) is responsible for the chicken muscular dystrophy. *FEBS lett*. 2008;582(15):2212-2218.
7. Nakamura N. Dystrophy of the diaphragmatic muscles in Holstein-Friesian steers. *J Vet Med Sci*. 1996;58(1):79-80.
8. van Lunteren E, Moyer M, Leahy P. Gene expression profiling of diaphragm muscle in alpha2-laminin (merosin)-deficient dy/dy dystrophic mice. *Physiol Genomics*. 2006;25(1): 85-95.
9. van Vleet JF, Valentine BA. Muscle and tendon. In: Maxie MG, ed. *Jubb, Kennedy, and Palmer's Pathology of Domestic Animals*. Vol 1. 5th ed. Philadelphia, PA: Elsevier Limited; 2007:210-216.
10. Wang Z, Chamberlain JS, Tapscott SJ, Storb R. Gene therapy in large animal models of muscular dystrophy. *ILAR J*. 2009;50:187-198.
11. Willmann R, Possekel S, Dubach-Powell J, Meier T, Ruegg MA. Mammalian animal models for Duchenne muscular dystrophy. *Neuromuscul Disord*. 2009;19: 241-249.

**CASE II: 161 2A (JPC 4003041).**

**Signalment:** Adult male crested-wood partridge, (*Rollulus rouloul*).

**History:** This bird was found dead on the floor of its enclosure. It had recently been the target of increased conspecific aggression.

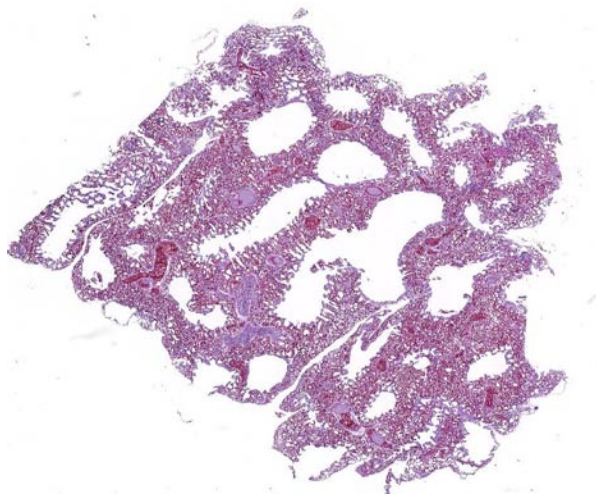
**Gross Pathology:** The skull was crushed with loss of overlying skin and soft tissues. The dorsal aspects of the cerebral hemispheres and cerebellum were exposed, lacerated and hemorrhagic. Fragments of brain tissue were embedded in bone at the fracture sites.

**Histopathologic Description:** Lungs: Throughout the section, pulmonary arterioles are diffusely congested and filled by variably sized, fragmented sections of neuropil sparsely populated by neurons, supportive glial cells and capillaries (gray matter) while others contain sections of white matter, portions of the molecular layer and granular layer separated by large multipolar Purkinje cells (cerebellum). In some sections there is a focal aggregate of macrophages, multinucleated giant cells and fewer lymphocytes and plasma cells that surround a central area of necrosis (granuloma). There are multifocal aggregates of macrophages that contain both fine black pigmented (carbon) and slightly larger, crystalline-like birefringent particulate debris associated with the parabronchi (anthracosis).

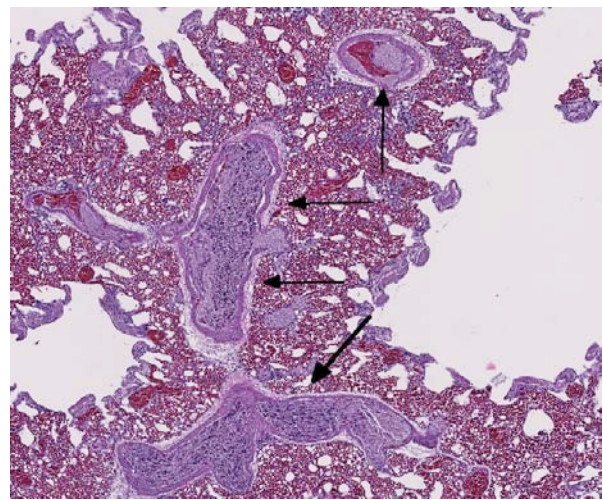
**Contributor's Morphologic Diagnosis:** Lungs:  
1) Brain tissue emboli, pulmonary arterioles, multifocal, peracute, moderate to severe with arteriolar congestion.  
2) Pneumonia, granulomatous, multifocal, chronic, mild (not present in all sections).  
3) Anthracosis, parabronchial, chronic, multifocal, mild.

**Contributor's Comment:** This crested wood partridge died from severe head trauma that resulted in fracture of the skull and disruption of the dorsal venous sinus and subjacent cerebrum and cerebellum. This severe trauma resulted in embolization of fragments of brain tissue that are visible throughout the pulmonary arterioles. The small granuloma present in one of the lungs was fungal in origin. Anthracosis is an exceedingly common finding in animals that inhabit densely populated urban environments. In this case, fungal pneumonia and anthracosis were mild and incidental to the death of this bird.

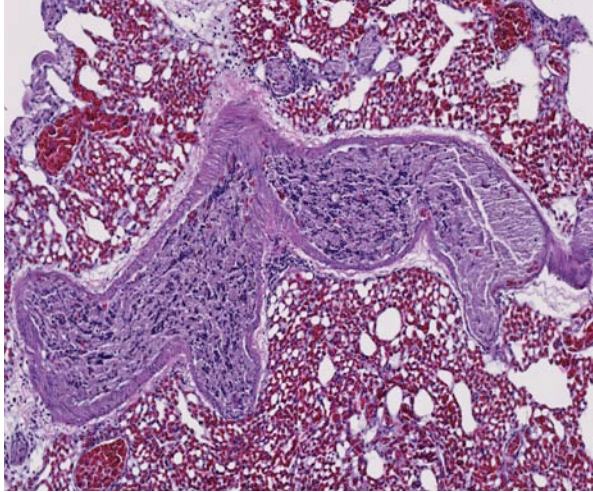
Cerebral tissue pulmonary embolization (CTPE) is a possible sequel to severe penetrating or closed head trauma. CTPE is most commonly associated with high impact blunt force trauma (i.e. automobile collision) in adults and instrument-assisted delivery in neonates.<sup>4,5</sup> Though a rare occurrence, post-traumatic pulmonary emboli can cause significant mortality (up to 43%) in the absence of prophylactic treatment.<sup>6</sup> Massive CTPE is detectable at autopsy and is associated with disruption of the large dorsal cerebral venous sinus in addition to brain injury. Microscopic brain emboli, however, have been identified in



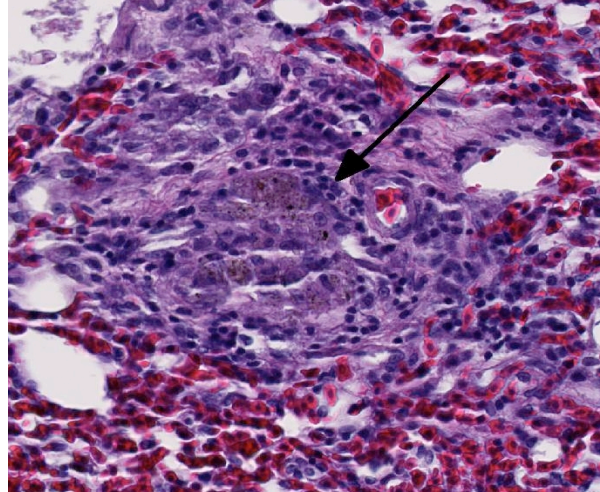
2-1. Lung, partridge: Several pulmonary arterioles contain eosinophilic material. (HE 0.63)



2-2. Lung, partridge: Higher magnification demonstrates neural tissue occluding several pulmonary arteries (arrows). (HE 34X)



2-3. Lung, partridge: Cerebral grey matter occludes a pulmonary arteriole. (HE 116X)



2-4. Lung, partridge: Adjacent to airways, granulomas surround black anthracotic pigment. (HE 248X)

pulmonary arterioles and systemic veins in cases with intact dura, suggesting embolic entry through smaller cerebral and meningeal veins.<sup>8</sup>

The behavior, physiology and anatomy of flighted birds may increase the likelihood of CTPE in avian species compared to terrestrial animals. Behaviorally, flighted birds are prone to severe brain trauma due to in-flight speed and prevalent collision injuries. Physiologically, avian veins, unlike mammalian veins, are compliance vessels, and they actively dilate during flight to increase cardiac output.<sup>9</sup> A larger venous diameter permits embolization of larger tissue fragments to the lungs. Anatomically, the avian brain and spinal cord are surrounded by a series of contiguous venous sinuses including the dorsal cerebral, occipital and vertebral sinuses and the ventral sinus cavernosus. These sinuses drain blood to the heart via the jugular or vertebral veins.<sup>10</sup> These extensive, superficial structures are prone to rupture with severe, closed or penetrating head trauma, presenting direct venous access to injured neural tissue.

This case illustrates dissemination of central nervous system (CNS) tissue to the venous system after head trauma. Consumption of meat products contaminated with CNS tissue from cattle with bovine spongiform encephalopathy is considered to be a significant route of transmission for mutant proteinase-resistant protein (PrP<sup>sc</sup>), the proposed etiologic agent of variant Creutzfeldt–Jakob disease (vCJD) in humans.<sup>2,7</sup> Air-injection penetrating captive bolt stunning prior to terminal

exsanguination has been identified as a major risk factor in CNS contamination of meat products. This method allows dislodged CNS tissue to disseminate through the bloodstream during the brief period of sustained cardiac function, followed by contamination of skeletal muscle with jugular exsanguination. For this reason, this method of cattle slaughter is currently banned in the United States and the European Union.<sup>1</sup>

**JPC Diagnosis:** 1. Lung, pulmonary arteries: Neural emboli, multiple.  
2. Lung: Granulomas, parabronchiolar, multiple, with anthracosis.

**Conference Comment:** The contributor provides an outstanding review of cerebral tissue pulmonary embolization. Both cerebral and cerebellar tissue was identified in emboli. This particular case has significant slide variation; in several sections the neural emboli are not as striking; however, immunohistochemical staining with GFAP confirms the presence of cerebrum or cerebellum within numerous pulmonary arterioles.

Conference participants conducted an abbreviated discussion of the anatomy and physiology of the normal avian lung. The avian mesobronchus (similar to the mammalian bronchus) is an airway lined with ciliated respiratory epithelium that has hyaline cartilage and smooth muscle within its walls; it has no direct function in gas exchange. The mesobronchus gives rise to the recurrent secondary bronchi, which are analogous to

mammalian bronchioles and contain smooth muscle, but no cartilage within their walls. These further divide into tertiary bronchi (parabronchi) with walls that are "scaloped" by bay-like air vesicles, where gas exchange takes place. Air vesicles are composed of simple squamous epithelium with an underlying supporting connective tissue. Air passes through numerous air capillaries in the wall of each air vesicle; these are adjacent to the blood capillaries, an arrangement that results in the establishment of a countercurrent flow. Unlike mammalian ventilation, in which a part of the ventilator volume is "stale" air, and mammalian structure with its numerous blind alleys and abundant dead space, the avian lung is a continuous flow system. Thus, avian lungs are much more efficient than mammalian, which is not surprising, considering the high demand of flight muscles for oxygenation.<sup>3</sup>

Participants closed with a brief summary of other reported causes of pulmonary emboli, including trophoblastic emboli (especially in guinea pigs), fibrocartilaginous emboli, neoplastic cells (especially lymphocytes in mice with tumor lysis syndrome), bone marrow elements (subsequent to injury/fracture), and allantoic fluid (in humans).

**Contributing Institution:** Wildlife Conservation Society  
Global Health Program - Pathology and Disease Investigation  
2300 Southern Blvd  
Bronx, NY 10460  
www.wcs.org

**References:**

1. Bowling MB, Belk KE, Nightingale KK, Goodridge LD, Scanga JA, Sofos JN, et al. Central nervous system tissue in meat products: an evaluation of risk, prevention strategies, and testing procedures. *Adv Food Nutr Res.* 2007;53:39-64.
2. Brown P, Will RG, Bradley R, Asher DM, Detwiler L. Bovine spongiform encephalopathy and variant Cruetzfeldt-Jakob disease: background, evolution and current concerns. *Emerg Infect Dis.* 2001;7:6-16.
3. Caceci T. Virginia-Maryland Regional College of Veterinary Medicine, Blacksburg, VA. VM8054 Veterinary Histology website. Respiratory System II: Avians. <http://www.vetmed.vt.edu/education/>

Curriculum/VM8054/Labs/Lab26/lab26.htm. Accessed February 22, 2014.

4. Cox P, Silvestri E, Lazda E, Nash R, Jeffrey I, Ostojic N et al. Embolism of brain tissue in intrapartum and early neonatal deaths: report of 9 cases. *Pediatr Dev Pathol.* 2009;12:464-468.
5. Echeverria RF, Baitello AL, Pereira de Godoy JM, Espada PC, Morioka RY. Prevalence of death due to pulmonary embolism after trauma. *Lung India.* 2010;27:72-74.
6. Geerts WH, Code KI, Jay RM, Chen E, Szalai JP. A prospective study of venous thromboembolism after major trauma. *N Engl J Med.* 1994;331:1601-1606.
7. Jones M, Peden AH, Prowse CV, Gröner A, Manson JC, Turner ML, et al. In vitro amplification and detection of variant Creutzfeldt-Jakob disease PrPSc. *J Pathol.* 2007;213:21-26.
8. Morentin B, Biritxinaga B. Massive pulmonary embolization by cerebral tissue after head trauma in an adult male. *Am J Forensic Med Pathol.* 2006;27:268-270.
9. Smith FM, West NH, Jones DR. The Cardiovascular system. In: Whittow GC, ed. *Sturkie's Avian Physiology.* 5th ed. San Diego, CA: Academic Press; 2000:174.
10. West NH, Langille BL, Jones DR. Cardiovascular system. In: King AS, McLelland J, eds. *Form and Function in Birds.* Vol. 2. San Francisco, CA: Academic Press; 1981:278-283.



**CASE III: JPC WSC #2 (JPC 4025665).**

**Signalment:** 13-week-old male Sprague-Dawley CD/IGS rat, (*Rattus norvegicus*).

**History:** Rats were necropsied 24 hours following two daily oral gavage doses of a test article.

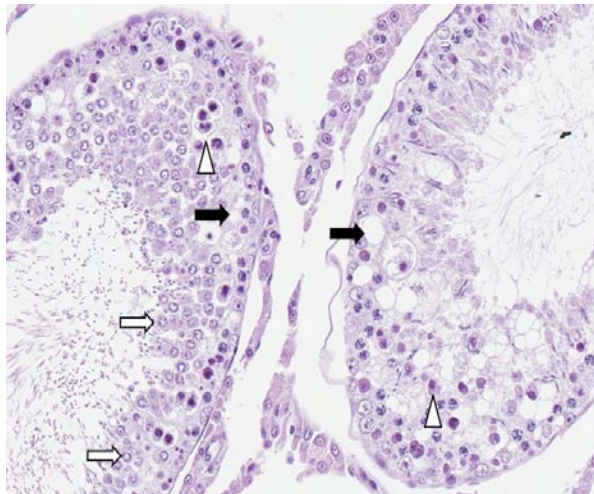
**Gross Pathology:** There were no notable gross observations.

**Histopathologic Description:** Many seminiferous tubule profiles, both early-stage and late-stage, have abnormal features including Sertoli cell vacuolation and germ cell degeneration, disorganization and depletion. Features of germ cell degeneration/necrosis include individual necrotic/apoptotic cells (especially spermatocytes); round spermatids with condensed and marginated nuclear chromatin and sometimes with excessive lightly basophilic granular cytoplasm or forming multinucleated giant cell syncytia. Some late-stage tubules have elongated spermatids with wavy, bent, or folded heads.

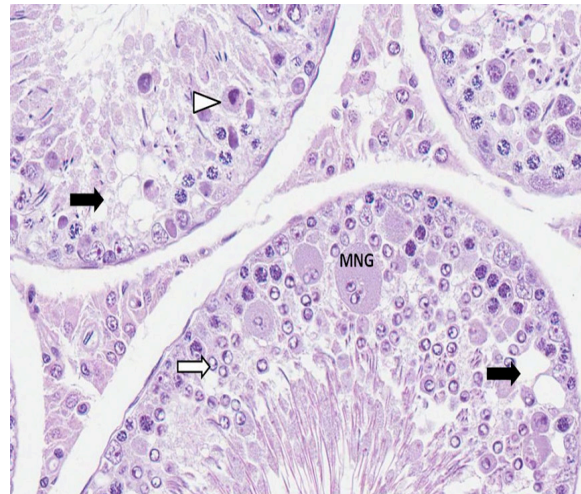
**Contributor's Morphologic Diagnosis:** Testis, seminiferous tubule: Germ cell degeneration/necrosis and Sertoli cell vacuolation, acute, diffuse, marked.

**Contributor's Comment:** The case provides an example of testicular injury 48 hours following treatment with 1,3-dinitrobenzene (1,3-DNB), a chemical intermediate formed during manufacture of many chemical compounds and a robust testicular toxicant in rodents.<sup>3</sup> Testicular toxicity is thought to be mediated by a reactive intermediate, 3-Nitrosanitrobenzene, formed during the reduction of 1,3-DNB to nitroaniline.<sup>1,3</sup> The Sertoli cell is thought to be the primary target cell of toxicity since ultrastructural changes in Sertoli cells have been shown to precede germ cell changes.<sup>3</sup> Sertoli cell vacuolation followed by degeneration of pachytene spermatocytes occur within the first 12 to 24 hours after administration of toxic doses and are reported to initially affect selected late stage tubules preferentially.<sup>3,4</sup> In the submitted case, 48 hours following exposure to the toxin, damage is more widespread across stages of the spermatogenic cycle and includes changes to early-stage as well as late-stage tubules. Tubular atrophy is a common sequel to the acute degenerative changes resulting from a single oral toxic dose of 1,3-DNB and may become apparent within about three weeks, though tubular regeneration and recovery may occur.<sup>4</sup>

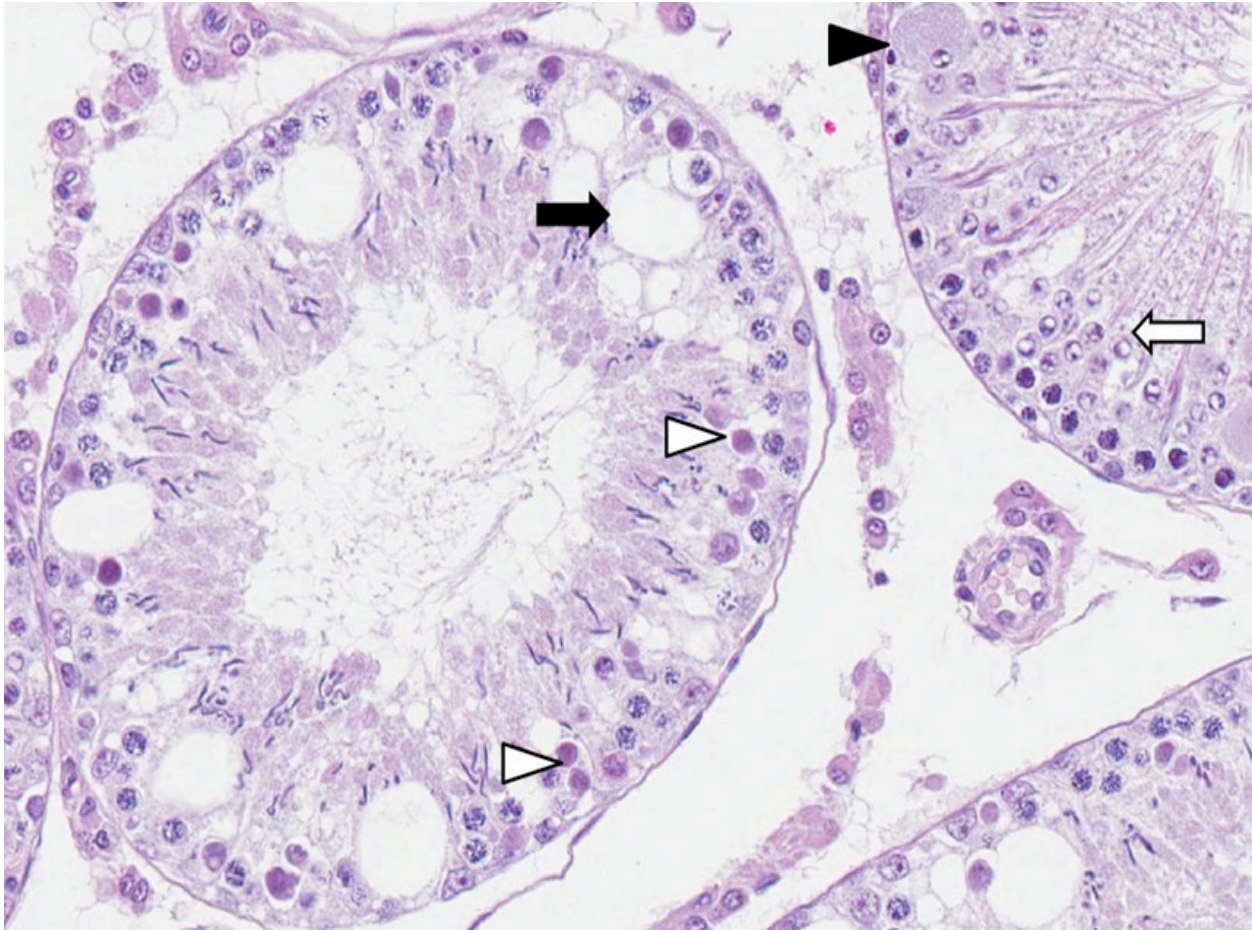
The severity of testicular damage induced by 1,3-DNB increases with age in rodents, and the proportion of early-stage tubules exhibiting



3-1. Testis, rat: Early (left) and late (right) stage tubule exhibiting Sertoli cell vacuolation (black arrow), spermatocyte necrosis (white arrowhead), and round spermatid marginated chromatin (white arrow). Disorganization and loss of germ cells is evident in both tubules but particularly in the late-stage tubule. (Photo courtesy of: Eli Lilly and Company, Department of Pathology and Toxicology, Indianapolis, IN 46285 www.lilly.com)



3-2. Testis, rat: Early stage tubule (bottom) and late-stage tubule (upper left). Multinucleated giant cell round spermatids (MNG), Sertoli cell vacuolation (black arrow), spermatocyte necrosis (white arrowhead), and round spermatid marginated chromatin (white arrow). Disorganization and loss of germ cells is evident in both tubules but particularly in the late-stage tubule. (Photo courtesy of: Eli Lilly and Company, Department of Pathology and Toxicology, Indianapolis, IN 46285 www.lilly.com)



3-3. Testis, rat: Late (left) and early (right) stage tubules. Sertoli cell vacuolation (black arrow), necrotic spermatocytes (white arrowhead), giant cell round spermatid (black arrowhead), round spermatid marginated chromatin (white arrow). Many elongated spermatids in the late-stage tubule have misshapen (wavy or bent) heads. (Photo courtesy of: Eli Lilly and Company, Department of Pathology and Toxicology, Indianapolis, IN 46285 www.lilly.com)

significant injury was shown to be notably higher in 120 day-old compared to 75 day-old rats.<sup>1</sup> Differences in susceptibility to testicular toxicity are thought to be related to differences in rates of hepatic clearance and intratesticular metabolism.<sup>1</sup> Methemoglobinemia, anemia, and liver injury are features of 1,3-DNB toxicity in humans; a literature search did not identify citations confirming that testicular injury is recognized in humans.

**JPC Diagnosis:** Testicle, seminiferous tubules: Degeneration, multifocal, moderate, with Sertoli cell vacuolation, spermatocyte degeneration and necrosis and multinucleate spermatid formation.

**Conference Comment:** Spermatogenesis results from a complex interaction between various hormones, germ cells, Sertoli cells and interstitial (Leydig) cells. Luteinizing hormone (LH)

released from the pituitary gland binds LH receptors on Leydig cells, inducing the production of testosterone, which binds to receptors on Sertoli cells (and possibly germ cells). Testosterone has also been shown to inhibit germ cell apoptosis, a normal method of regulating the cell population. Follicle-stimulating hormone (FSH) from the pituitary gland directly stimulates Sertoli cells (and possibly germ cells), while inhibin, produced by Sertoli cells, is a negative feedback mechanism that inhibits FSH production. During spermatogenesis, germ cells pass through spermatogonia, spermatocyte and spermatid stages.<sup>2</sup> In the rat, spermatogenesis is divided into 19 stages.<sup>5</sup> Spermiation is the active release of spermatozoa by Sertoli cells into the lumen. Sertoli cells, the support cells of the seminiferous tubule, maintain tubular epithelial integrity, phagocytose apoptotic germ cells, secrete fluid and proteins, regulate

spermatogenesis, metabolize steroids, provide nutrients to germ cells, and mediate hormonal effects on the germ cells. Furthermore, occluding junctions of Sertoli cells form an important part of the blood-testis barrier.<sup>2</sup> Thus, damage to Sertoli cells can also result in degenerative changes in the germ cell line, as demonstrated in this case.

The moderator additionally offered several recommendations for performing testicular and epididymal evaluation in the rat, including: a) using Bouin's or Modified Davidson's solution for fixation; histochemical staining with PAS-Hematoxylin to highlight the acrosome (this does not work in dogs); and performing a "stage-aware" assessment of seminiferous tubules using species-specific spermatogenesis chart.

**Contributing Institution:** Eli Lilly and Company  
Department of Pathology and Toxicology  
Indianapolis, IN 46285  
www.lilly.com

**References:**

1. Brown CD, Forman CL, McEuen SF, Miller MG. Metabolism and testicular toxicity of 1,3-dinitrobenzene in rats of different ages. *Fundam Appl Toxicol.* 1994;23:439-446.
2. Foster RA, Ladds PW. Male genital system. In: Maxie MG, ed. *Jubb, Kennedy, and Palmer's Pathology of Domestic Animals*. Vol. 3. 5th ed. Philadelphia, PA: Elsevier Limited; 2007:566-567.
3. Foster PMD, Sheard CM, Lloyd SC. 1,3-Dinitrobenzene: a Sertoli Cell toxicant? In: Stefanini M, Conti M, Geremia R, Ziparo E, eds. *Molecular and Cellular Endocrinology of the Testis*. New York, NY: Elsevier Science Publishers; 1986:281-288.
4. Hess RA, Linder RE, Strader LF, Perreault SD. Acute effects and long-term sequelae of 1,3-dinitrobenzene on male reproduction in the rat I. Quantitative and qualitative histopathology of the testis. *J Androl.* 1988;9:327-342.
5. Russell LD, Ettlin RA, Sinha Hikim AP, Clegg ED. *Histological and Histopathological Evaluation of the Testis*. Clearwater, FL: Cache River Press; 1990:65.

**CASE IV: A543/405/223-13 (JPC 4035678).**

**Signalment:** 3-week-old broiler chicken, (*Gallus gallus domesticus*).

**History:** There was a sudden onset of mortality affecting 10% of the flock. Sick birds adopted a crouching position with ruffled feathers and died within 48 hours.

**Gross Pathology:** At necropsy, diffuse yellowish-pale, friable and swollen livers are seen. Multiple petechiae beneath the capsule are present in some livers.

**Histopathologic Description:** There is a disruption of the hepatic parenchyma due to the presence of multifocal to coalescing randomly distributed foci of degenerated hepatocytes. These hepatocytes are swollen with hypereosinophilic and highly vacuolated cytoplasm, and a pyknotic nucleus with karyorrhexis and/or karyolysis. Associated with these foci and randomly scattered throughout the

parenchyma are hepatocytes with marked karyomegaly, chromatin condensation at the nuclear membrane and large basophilic intranuclear inclusion bodies. There is a moderate lymphoplasmacytic and heterophilic inflammatory infiltrate in the periportal areas. Diffuse cytoplasmic vacuolation is observed within remaining hepatocytes. Occasionally, there is focal widening and infiltration of sinusoids with lymphocytes, heterophils and histiocytes.

**Contributor's Morphologic Diagnosis:** Liver: Acute, severe, multifocal to coalescing necrotizing hepatitis with intranuclear inclusion bodies in hepatocytes.

**Contributor's Comment:** Inclusion body hepatitis (IBH) is a viral disease produced by a member of the family *Adenoviridae*, genus *Aviadenovirus*,<sup>1</sup> which was first described in chickens by Helmboldt and Frazier in 1963.<sup>3</sup> IBH is a ubiquitous disease in commercial and farm birds,<sup>1</sup> although recently infection has also been



4-1. Liver, broiler chicken: At necropsy, the liver is swollen, yellow, and friable. (Photo courtesy of: Servei de Diagnostic de Patologia Veterinaria, Facultat de Veterinaria, Bellaterra (Barcelona), Zip/Postal Code: 08193 SPAIN)

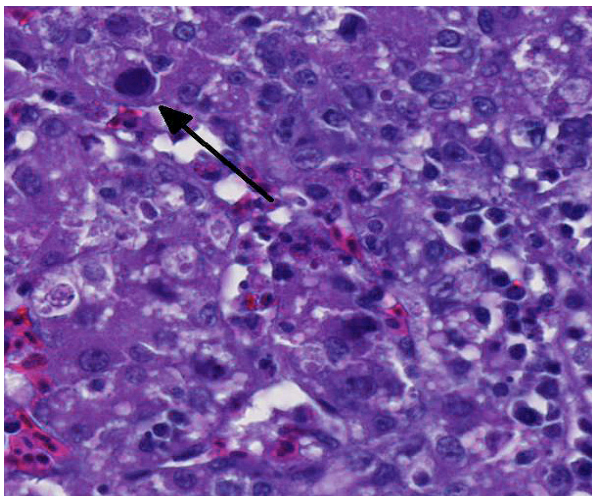
demonstrated in wild and exotic birds, producing the same characteristic hepatic lesions.<sup>5</sup>

The liver is the primary organ affected.<sup>1</sup> The infection produces a multifocal necrotizing hepatitis with intranuclear inclusion bodies in the hepatocytes.<sup>1,6</sup> Within the literature, the description of these intranuclear inclusion bodies is variable; inclusions have been described as large and eosinophilic or basophilic, or irregularly shaped, but they always replace/peripherally displace chromatin, and produce significant karyomegaly.<sup>1</sup>

**JPC Diagnosis:** Liver: Hepatitis, necrotizing, diffuse, severe, with numerous hepatocellular intranuclear viral inclusions.

**Conference Comment:** Although tissue sections are somewhat poorly preserved, the characteristic microscopic features, including the presence of viral inclusions with corresponding karyomegaly and peripheralization of chromatin, are nicely demonstrated in this case. Furthermore, the image of the affected liver submitted by the contributor provides an excellent example of the gross findings classically associated with IBH in chickens.

Members of the family *Adenoviridae* are non-enveloped, icosahedral, dsDNA viruses composed of four genera: *Aviadenovirus* (infects birds), *Mastadenovirus* (infects mammals), *Atadenovirus* (infects birds, mammals and reptiles) and



4-2. Liver, broiler chicken: At the edges of necrotic areas, hepatocellular nuclei are often expanded by a large basophilic adenoviral inclusion. Degenerating hepatocytes contain numerous cytoplasmic lipid droplets. (HE 360X)

*Siadenovirus* (infects birds, amphibians, reptiles); there is also a proposed fifth genus that includes adenoviruses of fish, such as white sturgeon adenovirus. Adenoviruses characteristically produce viral inclusion bodies within the host cell nucleus, where replication occurs.<sup>4</sup> Readers are urged to review WSC 2009-2010, Conference 9, case 3 for additional details regarding general characteristics of adenoviruses. See table 1 for a summary of select adenoviruses significant in veterinary medicine.

Important aviadenoviruses (subgroup I) include inclusion body hepatitis virus, quail bronchitis virus and hydropericardium syndrome virus. Turkey adenovirus 3, the causative agent of hemorrhagic enteritis in turkeys, marble spleen disease in pheasants and avian adenovirus splenomegaly in broilers, is a siadenovirus (subgroup II), while egg drop syndrome virus is a member of the genus *Atadenovirus* (subgroup III).<sup>1</sup> The pathogenesis of subgroup I avian adenoviruses is less defined than that of subgroups II and III; however, in general, both vertical and horizontal (especially fecal-oral) transmission are thought to be important in all aviadenoviruses. As noted by the contributor, IBH virus primarily targets hepatocytes, but pancreatic lesions are reported as well. Infection tends to occur in 3-7 week old broiler chickens (although it has been reported in birds as young as 7 days and as old as 20 weeks) resulting in up to 30% mortality. It often occurs as a secondary infection in immunodeficient birds with other diseases, predominantly infectious bursal disease (birnavirus, serotype 1) and chicken infectious anemia (circovirus). Outbreaks of IBH with similar gross and histological lesions have also been reported in columbiformes, psittacines and raptors.<sup>1</sup>

The recently identified falcon adenovirus, which is distantly related to fowl adenovirus types 1 and 4 (see WSC 2007-2008, Conference 23, case 3) rarely causes necrotizing hepatitis and splenitis with characteristic intranuclear viral inclusions; stress related to shipping or breeding is a likely predisposing factor for clinical disease.<sup>2</sup> Quail bronchitis virus, caused by avian adenovirus 1, is a worldwide disease of both captive and wild bobwhite quail; birds present with respiratory distress, nasal discharge, coughing, sneezing, conjunctivitis and, occasionally in older birds,

diarrhea. Mortality approaches 100% in the young, but falls below 25% in those older than 4 weeks. Microscopic findings include tracheitis, air sacculitis and enteritis, with characteristic intranuclear viral inclusions. Infection with fowl adenovirus type 4 is believed to be the cause of hydropericardium syndrome virus (Angara disease), which is found in the Middle East as well as South America; particularly severe manifestations are also associated with immunosuppression. Lesions include pericardial effusion, pulmonary edema, hepatomegaly and renomegaly; mortality can range from 20-80%; and affected broilers are usually 3-5 weeks old.<sup>4</sup>

Egg drop syndrome, an atadenovirus (subgroup III) recognized in chickens, ducks and geese results in the production of soft-shelled or shell-less eggs. It is suspected that the virus originated in ducks and was passed to chickens via contaminated Marek's disease vaccine produced with duck embryo fibroblasts; spread within flocks occurs through contaminated eggs, droppings and fomites. Egg drop syndrome has worldwide distribution except the United States and Canada. The siadenovirus (subgroup II), turkey adenovirus 3, produces splenomegaly, hemorrhagic enteritis and immunosuppression with secondary opportunistic infections in turkeys older than 4 weeks. A serologically identical virus also causes marble spleen disease in pheasants and splenomegaly in chickens. Microscopic lesions are similar in all species and include splenic reticuloendothelial hyperplasia with intranuclear viral inclusions and fibrinonecrotic, hemorrhagic enteritis. There is a vaccine available.<sup>4</sup>

Table 1: Select adenoviruses in veterinary species.<sup>1,4</sup>

Species	Name	Comment
Dogs	Canine adenovirus 1 Canine adenovirus 2 (mastadenovirus)	- Infectious canine hepatitis - Infectious canine tracheobronchitis
Horses	Equine adenovirus 1 & 2 (mastadenovirus)	- Asymptomatic or mild respiratory disease in immunocompetent hosts - Bronchopneumonia/systemic disease in Arabian foals with SCID

Cattle	Bovine adenovirus (mastadenovirus and atadenovirus)	- 10 serotypes - Asymptomatic or mild respiratory disease - Occasionally pneumonia, enteritis, keratoconjunctivitis in calves
Swine	Porcine adenovirus (mastadenovirus)	- 4 serotypes - Asymptomatic or mild respiratory disease/enteritis; rarely encephalitis
Sheep	Ovine adenovirus (mastadenovirus and atadenovirus)	- 7 serotypes - Asymptomatic or mild respiratory disease - Occasionally severe respiratory/enteric disease in lambs
Goats	Caprine adenovirus (mastadenovirus and atadenovirus)	- 2 serotypes - Asymptomatic or mild respiratory disease
Deer	Cervine adenovirus (Odocoileus adenovirus 1; atadenovirus)	- Vasculitis, hemorrhage, pulmonary edema
Rabbits	Adenovirus 1 (mastadenovirus)	- Diarrhea
Mice	Murine adenovirus 1 & 2 (mastadenovirus)	- Murine adenovirus 1: experimental infections - Murine adenovirus 2: enterotropic; causes runtting in neonates
Guinea pigs	Guinea pig adenovirus (mastadenovirus)	- Usually asymptomatic; rarely pneumonia with high mortality, low morbidity
Chickens	Fowl adenovirus (aviadenovirus, atadenovirus and siadenovirus)	- 12 serotypes of aviadenovirus (inclusion body hepatitis, hydropericardium syndrome) - 1 serotype of atadenovirus (egg drop syndrome) - 1 serotype of siadenovirus (adenovirus-associated splenomegaly)

Turkeys	Turkey adenovirus 1-3 (siadenovirus and aviadenovirus)	- turkey adenovirus 3, siadenovirus (hemorrhagic enteritis, egg drop syndrome) - turkey adenovirus 1 & 2, aviadenovirus (depressed egg production)
Quail	Avian adenovirus 1 (aviadenovirus)	- 1 serotype, aviadenovirus (bronchitis)
Pheasants	- serologically indistinguishable from Turkey adenovirus 3 (siadenovirus)	- Siadenovirus (marble spleen disease)
Ducks	Duck adenovirus 1 & 2 (atadenovirus and aviadenovirus)	- 1: atadenovirus (asymptomatic or drop in egg production) - 2: aviadenovirus (rare hepatitis)

**Contributing Institution:** Servei de Diagnòstic de Patologia Veterinària  
Facultat de Veterinària  
Bellaterra (Barcelona), 08193 Spain

**References:**

1. Adair BM, Fitzgerald SD. Group I adenovirus infections. In: *Diseases of Poultry*. 12th ed. Ames, IA: Iowa State Press; 2008:252-266.
2. Dean J, Latimer KS, Oaks JL, Schrenzel M, Redig PT, Wünschmann A. Falcon adenovirus infection in breeding Taita falcons (*Falco fasciinucha*). *J Vet Diagn Invest*. 2006;18:282-286.
3. Hollell J, McDonald DW, Christian RG. Inclusion body hepatitis in chickens. *Can Vet J*. 1970;11:99-101.
4. MacLachlan NJ, Dubovi EJ. *Fenner's Veterinary Virology*. 4th ed. London, UK: Academic Press; 2011:203-212.
5. Ramis A, Marlasca MJ, Majo N, Ferrer L. Inclusion body hepatitis (IBH) in a group of Eclectus parrots (*Eclectus roratus*). *Avian Pathol*. 1992;21(1):165-169.
6. Randall CJ, Reece RL. *Color Atlas of Avian Histopathology*. Mosby-Wolfe, Times Mirror International Publishers Limited; 1996:95-96.